Bayesian Uncertainty Quantification in Seismically Isolated Structures Equipped with Nonlinear Hysteretic Devices

Costas Argyris, Panos Tsopelas, and Costas Papadimitriou

***Abstract*—Bayesian inference is used to quantify and propagate uncertainties in the parameters of nonlinear structural dynamics models of seismically isolated structures equipped with nonlinear hysteretic devices. The ultimate goal is to build high fidelity models of the system components to simulate the behavior (performance and reliability) of the combined system. The structural parameter calibration and uncertainty quantification are performed at the system level for the nonlinear hysteretic isolation devices using controlled laboratory tests performed on a shake table. Uncertainty models are identified using measurements for system tests, consisting of displacement, acceleration and restoring force response time histories. The model uncertainty analyses resulted in building a high fidelity model for the system that can be used for performing reliable robust performance predictions that properly take into account model uncertainties.**

I. Introduction

Bayesian inference is used for quantifying and calibrating uncertainty models in structural dynamics based on vibration measurements, as well as propagating these uncertainties in structural dynamics simulations for updating robust predictions of system performance, reliability and safety [1]. Asymptotic and stochastic simulation tools can be used to quantify and propagate uncertainties. Asymptotic formulations [2] are approximate and may miss-represent the posterior distribution of the model parameters for concave supports, multimodal or unidentifiable posterior distributions. They also require that the derivatives and hessians of measures of fit between the response quantities of interest (QoI) and corresponding measurements are available. Adjoint formulations, in particular, can be used to substantially reduce the computations related to estimating the sensitivities of the measures of fit with respect to the number of parameters. For nonlinear models of structures subjected to earthquake-like excitation, the adjoint formulation might not exist or may not be easily implemented in software. Stochastic simulation algorithms are more convenient to use since can better represent complex posterior distributions and do not require the estimation of derivatives of response quantities with respect to the model parameters.

Computationally intensive stochastic simulation algorithms (e.g. Transitional MCMC [3]) are well suited tools for identifying system and uncertainty models as well as performing robust prediction analyses. The stochastic simulation tools involve generating samples for tracing and then populating the important uncertainty region in the parameter space, as well as evaluating integrals over high-dimensional spaces of the uncertain model parameters by sample estimates. They require a very large number of system analyses to be performed over the space of uncertain parameters which may lead to excessive computational time. Consequently, the computational demands depend highly on the number of system analyses and the time required for performing a system analysis. This in turn depends on the complexity of the model of the analyzed system as well as the number of uncertain parameters involved. Efficient computing techniques have been integrated with the Bayesian framework to handle large-order models and localized nonlinear actions [4]. Specifically, surrogate models can be adopted to reduce the number of full system runs, and parallel computing algorithms can be used to efficiently distribute the computations in available multi-core CPUs [4]. Depending on the number of available computer workers, drastic reduction in computational effort to manageable levels can be achieved for models for which the time to execute one system simulation is of the order of several seconds, minutes or even hours.

This work is concerned with calibrating models of seismic isolated structures equipped with nonlinear isolator devices. Thus, the equations of motion are nonlinear due to the nonlinear models used for the isolator devices. Parameterized model structures of the isolator devices are introduced and the Bayesian framework is used to estimate the model parameter values and their associated uncertainties. The estimation is based on experimental data obtained by shake table tests on the combined bridge on isolators system. Calibration of the uncertainties in the model parameters is based on full response time histories predicted by the model and measured by a network of sensors. The Transitional Markov Chain Monte Carlo (TMCMC) algorithm [3] is used for identifying system and uncertainty models as well as performing robust prediction analyses are stochastic simulation algorithms. This algorithm is used to represent the posterior distribution of the parameters of the non-linear isolation system, as well as propagate this uncertainty to obtain the uncertainty in response quantities of interest. For nonlinear models of the type analyzed in this work, the time to execute one simulation of the system is of the order of a few seconds which poses moderate computational requirements. However, parallel computing algorithms [4] are used to efficiently distribute the computations in available multi-core CPUs, thus achieving further computational savings.

This work is organized as follows. Section II presents the Bayesian uncertainty quantification and propagation framework that is used to quantify uncertainties in the nonlinear models of the combined bridge-isolators system for the case where the measurements consist of response time histories. Section III. Section III introduces the bridge, the experimental setup, the

nonlinear model, including the models of the isolators, and the instrumentation used. Finally, the results of the uncertainty calibration are presented in Section IV. Conclusions of this work are summarized in Section V.

II. BAYESIAN UNCERTAINTY QUANTIFICATION AND PROPAGATION

A. *Parameter Estimation*

The Bayesian methodology [5, 6] is used to calibrate and estimate the uncertainties in the parameters appearing in the non-linear models describing the behavior of the bridge under seismic excitation, using measured response time histories of displacements, accelerations, and forces at different parts of the bridge. According to the methodology, if $\underline{\theta}$ denotes the vector of the parameters of the non-linear models, and $\underline{\sigma}$ denotes an additional set of prediction error parameters to be defined later, the uncertainty in these parameters given the measured data D is quantified by the posterior distribution that is obtained from Bayes' theorem as

$$p\left(\underline{\theta},\underline{\sigma} \mid D\right) = \frac{p\left(D \mid \underline{\theta},\underline{\sigma}\right)\pi\left(\underline{\theta},\underline{\sigma}\right)}{p\left(D\right)} \tag{1}$$

where $p\left(D \mid \underline{\theta},\underline{\sigma}\right)$ is the likelihood, $\pi\left(\underline{\theta},\underline{\sigma}\right)$ is the prior distribution of the uncertain parameters and $p\left(D\right)$ is the evidence of the model. The posterior distribution $p\left(\underline{\theta},\underline{\sigma} \mid D\right)$ quantifies the uncertainty in the model and prediction error parameters by measuring the plausibility of each possible set of parameters given the data D.

To apply the Bayesian formulation for parameter calibration of non-linear models, we consider that the data consists of measured time histories $D = \left\{\hat{x}_j\left(k\right) \in R,\ j = 1,\cdots,N_0,\ k = 1,\cdots,N_D\right\}$ at time instances $t = k\Delta t$, of N_0 response quantities (displacements, accelerations and forces) at different points in the bridge, where N_D is the number of the samples data using a sampling period Δt.

Let also $\left\{x_j\left(k;\underline{\theta}\right) \in R,\ j = 1,\ldots,N_0,\ k = 1,\ldots,N_D\right\}$ be the predictions of the response time histories for the same quantities and points in the structure, from the non-linear model corresponding to a particular value of the parameter set $\underline{\theta}$. The prediction error equation between the sampled response time history of the quantity j at time $t = k\Delta t$ and the corresponding response time history predicted from the model for a particular value of the parameter set $\underline{\theta}$ can now take the form

$$e_j\left(k\right) = \hat{x}_j\left(k\right) - x_j\left(k;\underline{\theta}\right) \tag{2}$$

where $j = 1,\ldots,N_0$ and $k = 1,\ldots,N_D$.

Prediction errors, measuring the fit between the measured and the model predicted response time histories, are modeled by Gaussian distributions. The difference between the measured and model predicted response is attributed to both experimental errors and modeling error. The prediction errors of a response time history at different time instants are assumed to be independent zero-mean Gaussian variables with equal variances for all sampling data of a response time history, but each time history is allowed to have a different prediction error associated with it. This formulation takes into account the fact that each measured time history is generally obtained from a different sensor (displacement, acceleration or force sensor) with a different accuracy and noise level, and this results in a number of prediction errors equal to the number of measured time histories.

Under the zero-mean Gaussian assumption for the prediction error, $e_j\left(k\right) \sim N\left(0,\sigma_j^2\right)$, the measured quantity $\hat{x}_j\left(k\right)$ also follows a Gaussian distribution with mean $x_j\left(k;\underline{\theta}\right)$ and variance σ_j^2, $\hat{x}_j\left(k\right) \sim N\left(x_j\left(k;\underline{\theta}\right),\sigma_j^2\right)$. In the analysis that follows, the prediction error parameters $\sigma_j,\ j = 1,\ldots,N_0$ are contained in the prediction error vector $\underline{\sigma} \in R^{N_0}$. The prediction error e_j provide a measure of the discrepancy between the measured and model predicted quantities. As already stated, this generally breaks down to two terms for the prediction error, one for the experimental error and one for the model error. In this study such a distinction is not made, and the prediction error is thought of as a measure of the total discrepancy between measurements and the model predictions without being able to distinguish how much is due to experimental or modeling error. Depending on the problem, and more specifically on the way the data was collected, $\underline{\sigma}$ might be considered known or unknown. In the most general case it is considered unknown and therefore is included in the parameters for calibration, along

with the structural model parameters. Herein, the prediction error parameters are considered unknown and from now on are included in the parameters to be calibrated given the data, along with the structural model parameters in the set $\underline{\theta}$.

The likelihood function $p\left(D \mid \underline{\theta}, \underline{\sigma}\right)$, which quantifies the probability of obtaining the data given a specific set of structural parameters and prediction error parameters, is derived by noting that the measured time histories $\hat{x}_j\left(k\right)$ are implied from (2) to be independent Gaussian variables with mean $x_j\left(k;\underline{\theta}\right)$ and variance σ_j^2. Taking advantage of the independence of the measured quantities both at different time instants of the same time history as well as between different time histories, the likelihood is formulated as follows.

$$p\left(D \mid \underline{\theta}, \underline{\sigma}\right) = \prod_{j=1}^{N_0} \prod_{k=1}^{N_D} p\left(\hat{x}_j\left(k\right) \mid \underline{\theta}, \underline{\sigma}\right) \tag{3}$$

Substituting with the formula for the Gaussian probability density function and rearranging terms one obtains that

$$p\left(D \mid \underline{\theta}, \underline{\sigma}\right) = \frac{1}{\left(\sqrt{2\pi}\right)^{N_D N_0} \prod_{j=1}^{N_0} \sigma_j^{N_D}} \exp\left\{-\frac{1}{2} \sum_{j=1}^{N_0} \frac{1}{\sigma_j^2} \sum_{k=1}^{N_D} \left[\hat{x}_j\left(k\right) - x_j\left(k;\underline{\theta}\right)\right]^2\right\} \tag{4}$$

Introducing the overall fit function

$$J\left(\underline{\theta};\underline{\sigma}\right) = \frac{1}{N_0} \sum_{j=1}^{N_0} \frac{1}{\sigma_j^2} J_j\left(\underline{\theta}\right) \tag{5}$$

where

$$J_j\left(\underline{\theta}\right) = \frac{1}{N_D} \sum_{k=1}^{N_D} \left[\hat{x}_j\left(k\right) - x_j\left(k;\underline{\theta}\right)\right]^2 \tag{6}$$

represents the measure of fit between the measured and the model predicted response time history for quantity j, the likelihood function can be compactly written in the form

$$p\left(D \mid \underline{\theta}, \underline{\sigma}\right) = \frac{1}{\left(\sqrt{2\pi}\right)^{N_D N_0} \prod_{j=1}^{N_0} \sigma_j^{N_D}} \exp\left\{-\frac{N_D N_0}{2} J\left(\underline{\theta};\underline{\sigma}\right)\right\} \tag{7}$$

Substituting (7) in (1) one derives the posterior probability distribution of the parameters in the form

$$p\left(\underline{\theta}, \underline{\sigma} \mid D\right) = \frac{\pi\left(\underline{\theta}, \underline{\sigma}\right)}{p(D)\left(\sqrt{2\pi}\right)^{N_D N_0} \prod_{j=1}^{N_0} \sigma_j^{N_D}} \exp\left\{-\frac{N_D N_0}{2} J\left(\underline{\theta};\underline{\sigma}\right)\right\} \tag{8}$$

Herein the Transitional MCMC [3] is used to draw samples from the posterior distribution.

B. Uncertainty Propagation

The main interest in updating the uncertainty in the model parameters through measured data lies in propagating this uncertainty through the model to quantify the uncertainty in output quantities of interest (QoI). Specifically, given a scalar output QoI $g\left(\underline{\theta}\right)$ which depends on the uncertain parameters $\underline{\theta}$, the objective is to evaluate its uncertainty given the uncertainty in $\underline{\theta}$ which is quantified by the posterior PDF in (8). Simple measures of uncertainty in $g\left(\underline{\theta}\right)$ are the mean, given by

$$Mean\left[g\left(\underline{\theta}\right)\right] = E\left[g\left(\underline{\theta}\right)\right] = \int g\left(\underline{\theta}\right) p\left(\underline{\theta} \mid D\right) d\underline{\theta} \tag{9}$$

and the variance, given by

$$Var\left[g\left(\underline{\theta}\right)\right] = E\left[g^2\left(\underline{\theta}\right)\right] - E^2\left[g\left(\underline{\theta}\right)\right] \tag{10}$$

where

$$E\left[g^2\left(\underline{\theta}\right)\right] = \int g^2\left(\underline{\theta}\right) p\left(\underline{\theta} \mid D\right) d\underline{\theta} \tag{11}$$

is the second moment of $g\left(\underline{\theta}\right)$.

Stochastic simulation algorithms are used to provide sample estimates of the integrals (9) and (11). Specifically, the Transitional Markov Chain Monte Carlo (TMCMC) algorithm [3] is used. The samples $\underline{\theta}^{(j)}$, $j = 1, \ldots, N$ drawn from the posterior PDF $p\left(\underline{\theta} \mid \mathrm{D}\right)$ can be used to approximate the integrals (9) and (11) with the sample estimates

$$E\left[g\left(\underline{\theta}\right)\right] \approx \frac{1}{N}\sum_{j=1}^{N} g\left(\underline{\theta}^{(j)}\right) \tag{12}$$

and

$$E\left[g^2\left(\underline{\theta}\right)\right] \approx \frac{1}{N}\sum_{j=1}^{N} g^2\left(\underline{\theta}^{(j)}\right) \tag{13}$$

The samples $\underline{\theta}^{(j)}$, $j = 1, \ldots, N$ are dependent, but are used for statistical averaging as if they were independent, accepting a reduced accuracy in the sample estimate.

III. Description of Model and Instrumentation

A. Description of Bridge and Isolation System

The physical system under examination is a scaled model of a bridge which was used to develop and test advanced sliding isolation systems for bridges (Fig. 1) [7]. The isolation system consists of flat sliding bearings, rubber restoring force devices and linear viscous fluid dampers. The bridge model is seismically excited on a shake table, and various response quantities are measured by an array of force, displacement and acceleration sensors located in different parts of the structure. The purpose of the isolation system is to prohibit certain response quantities from reaching critical values under seismic excitation. Fig. 2 shows a schematic diagram of the bridge model and the isolation system.

The studied isolation system consists of three components:

- Flat sliding bearings to support the weight of the deck and provide a mechanism for energy dissipation.
- Rubber devices for providing restoring force, that is, recentering capability.
- Linear viscous fluid dampers for enhancing the energy dissipation capability of the isolation system.

The three components of the isolation system provide load carrying capacity, restoring force capability (stiffness) and hysteretic and viscous damping which were not interrelated. The design requirements of the isolation system was to minimize the transmission of force to the substructure, that is piers and foundation, while bearing displacements in the scale of the model (length scale factor equal to 4) did not exceed 50 millimeters.

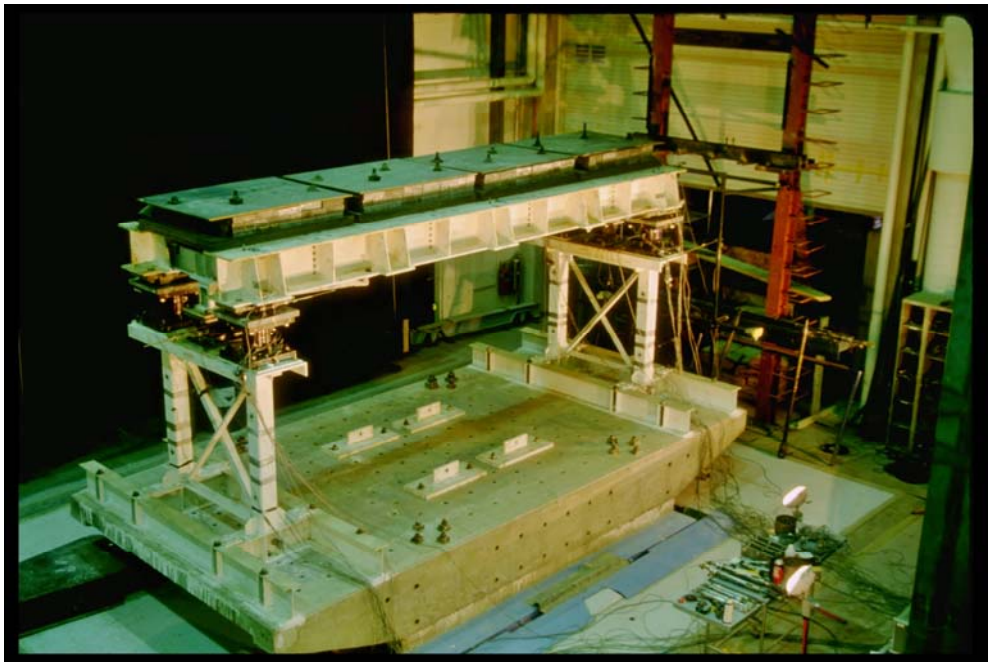

Figure 1. View of bridge model with isolation system.

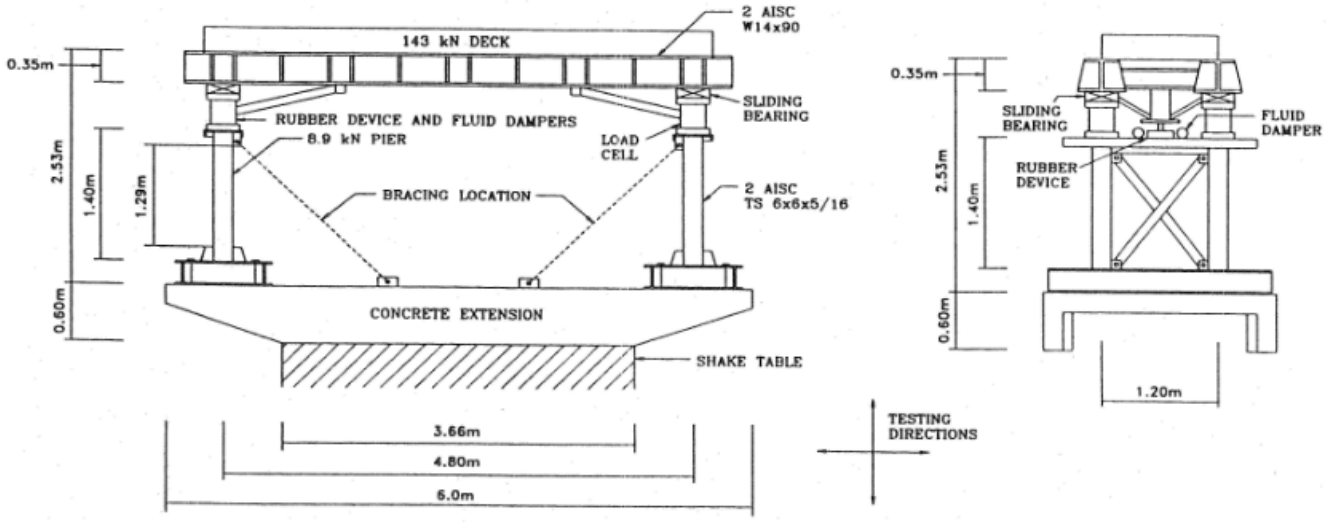

Figure 2. Schematic diagram of bridge model and isolation system.

B. Instrumentation

The instrumentation consisted of load cells, accelerometers, displacement transducers and strain gages. Fig. 3 shows a schematic diagram of the overall instrumentation, where the abbreviations stand for: A (acceleration), D (displacement), V-H-T (vertical-horizontal-transverse), D-P (deck-pier), E-W-N-S (east-west-north-south). Not all channels displayed in Fig. 3 were used for Bayesian parameter calibration. The bearing displacement was monitored by displacement transducers, while the pier shear force was measured by strain gages installed in the pier. The acceleration of the piers measured by accelerometers was also utilized in the Bayesian procedure. Finally, two quantities were not directly measured but rather inferred from other direct measurements. These two quantities were the pier drift and the pier isolator force. The pier drift was measured by subtracting the displacement at the bottom of the pier from the displacement at the top of the pier. The pier isolator force was calculated by adding the frictional force of the bearings (which was measured directly from load cells supporting the bearings) and the combined force from the rubber devices and fluid dampers. The previously mentioned direct and indirect measurements provided the experimental time histories which constitute the data set D, consisted of $N_0 = 5$ response time histories, introduced in the Bayesian formulation. The seismic excitation provided by the shake table was also

recorded in order to be used in the analytical model simulations. Details about the experimental setup and the analytical model can be found in [7].

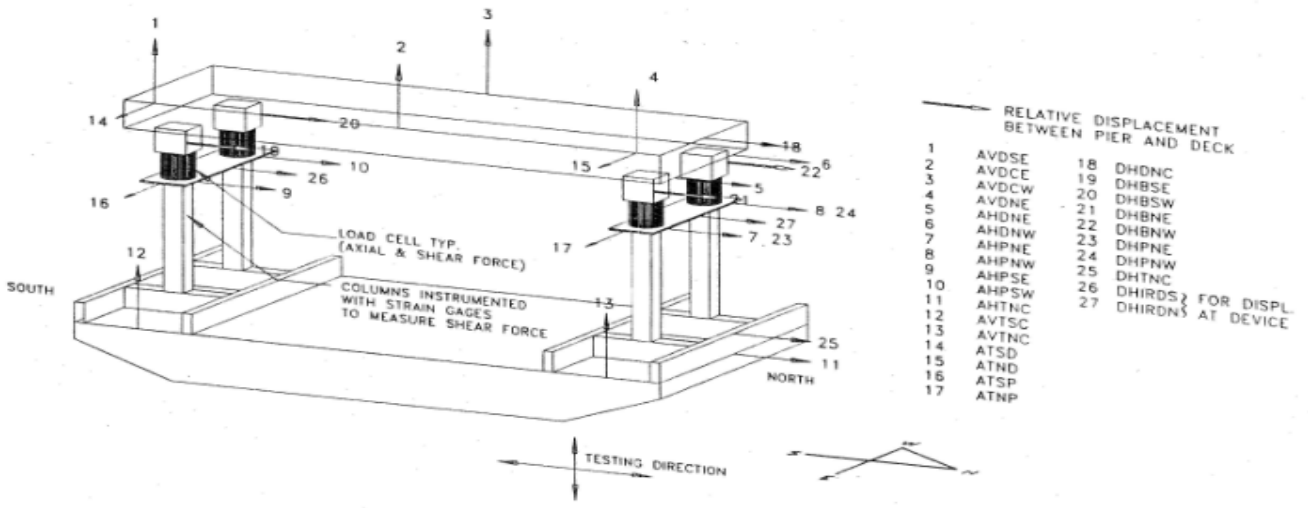

Figure 3. Overall instrumentation diagram.

C. Analytical Model

An analytical model was developed in order to predict the behavior of the bridge under different seismic excitations. The model predicts the time histories at locations where measurements are available, given the values of the parameters which appear in the nonlinear model equations. The analytical model accounts for the pier flexibility, pier top rotation, vertical motion effects on the properties of the sliding bearings, and nonlinear hysteretic characteristics of the restoring force devices. The degrees of freedom are selected to be the deck displacement with respect to the table, U_d, the pier displacements with respect to the table, U_{pi}, and the pier rotations, ϕ_{pi} (see Fig. 4). Each pier is modeled by a beam element of length L_i, moment of inertia I_i, and modulus of elasticity E_i, $i = 1, 2$. The beam element is fixed to the table and connected at its top to a rigid block of height h, mass m_{pi}, and mass moment of inertia about the center of mass I_{pi}. The center of mass is located at distance h_i from the bottom of the block. This block represents the pier top. The equations of motion are derived by consideration of dynamic equilibrium of the deck and piers in the horizontal direction and of the piers in the rotational direction. Free body diagrams of the deck and pier tops of the bridge model are shown in Fig. 4.

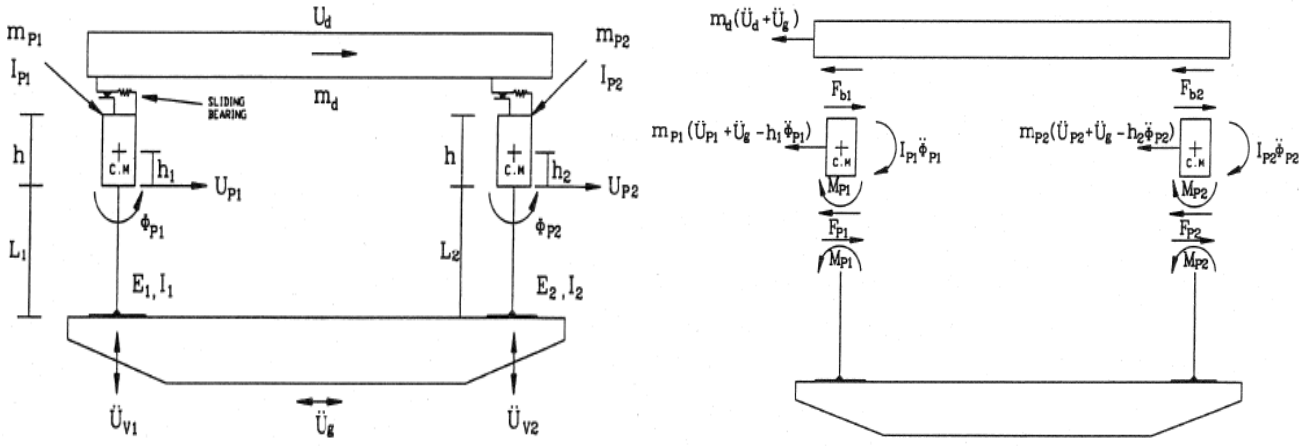

Figure 4. *Left:* Degrees of freedom of the analytical model. *Right:* Free body diagrams of deck and piers.

The dynamic equilibrium of forces includes the lateral forces in the isolation system which include friction in the sliding bearings, force from the restoring force devices and the forces from the fluid dampers. These forces are summarized in the total isolation system force as follows

$$F_{bi} = \mu_i \left(\dot{U}_{bi}\right) W_i + F_{ri}\left(U_{bi}\right) + nF_{di}\left(\dot{U}_{bi}\right) \tag{14}$$

where μ_i is the coefficient of sliding friction at pier i which is a function of the sliding velocity of the bearing $\dot{U}_{bi}$, W_i is the normal load on two sliding interfaces at pier i, F_{ri} is the restoring force from the rubber device at pier i, n is the number of fluid dampers at pier i, $\left(n=2\right)$ and F_{di} is the damping force of one fluid damper at pier i. The bearing displacement at pier i, U_{bi} is related to the model degrees of freedom with the geometrical relation

$$U_{bi} = U_d - U_{pi} + h\phi_{pi} \tag{15}$$

The coefficient of sliding friction in the sliding interface of the bearings followed the relation [7]

$$\mu_i = f_{\max,i} - (f_{\max,i} - f_{\min,i}) \exp\left(-a_i \left|\dot{U}_{bi}\right|\right) \tag{16}$$

where $f_{\max,i}$ is the coefficient of friction at high velocity of sliding in pier i, $f_{\min,i}$ is the coefficient of friction at essentially zero velocity of sliding in pier i, a_i is a parameter controlling the variation of the coefficient of friction with velocity of sliding and $\dot{U}_{bi}$ is the velocity of sliding. The parameters $f_{\max,i}$, $\Delta f = f_{\max,i} - f_{\min,i}$ and a_i for $i = 1, 2$ form the first six elements respectively of the uncertain parameter vector $\underline{\theta}$.

The rubber restoring force devices acted as horizontal springs with displacement restraint. They provide stiffness by deforming their inner rubber elements up to a point where the device exhibits increased stiffness and acts as a displacement restrainer. The maximum allowed displacement is 50 millimeters. The devices exhibited nearly linear behavior to displacements of about 35 millimeters. Beyond this limit they displayed increasing stiffness to the limit of about 50 millimeters. After that the devices exhibited nearly rigid behavior. Rubber devices were installed one at each pier location. Due to the non-linear force-displacement relationship of the rubber restoring force devices, higher order polynomials were used to model their behavior.

Specifically, the restoring force F_{ri} in the rubber device at pier i was described by two polynomials as follows

$$F_{ri} = F_{oi}\left(U_{bi}\right) + F_{Di}\left(U_{bi}\right) \tag{17}$$

where $F_{oi}\left(U_{bi}\right)$ is the displacement-dependent skeleton curve and $F_{Di}\left(U_{bi}\right)$ is, also displacement-dependent, the difference between the loading and unloading branches of the hysteresis loop of a rubber restoring force device. $F_{oi}\left(U_{bi}\right)$ and $F_{Di}\left(U_{bi}\right)$ may be expressed as odd and even polynomial functions of displacement, respectively

$$\begin{aligned} F_{oi} &= \sum_{n=1,3,5,\ldots}^{N} A_n U_{bi}^n \\ F_{Di} &= \sum_{m=0,2,4,\ldots}^{M} B_m U_{bi}^m \end{aligned} \tag{18}$$

where the coefficients of the polynomials, A_n and B_m could also be part of the uncertain parameter vector $\underline{\theta}$. In this study the values of these parameters are kept fixed to the values calibrated using component test measurements. Sufficiently good agreement with experimental force-displacement loops [7] was achieved by using $N = 11$ and $M = 4$. The values of the parameters obtained from the component tests were used as nominal values in the Bayesian procedure.

The third term in the right hand side of (14) is the force delivered by the fluid damper. The fluid viscous damper operates on the principle of fluid flow through orifices. The device consists of a stainless steel piston, with bronze orifice head and an accumulator. It is filled with silicone oil. Unlike typical fluid dampers which utilize cylindrical orifices, this device utilizes a series of specially shaped passages to alter flow characteristics with fluid speed. The damper was modeled using a Maxwell

arrangement of a purely elastic spring and a purely viscous dashpot connected in series. The force output F_{di} of the Maxwell model can be represented by the differential equation

$$\frac{\dot{F}_{di}}{K_{di}} + \frac{F_{di}}{C_{0i}} = \dot{U}_{bi} \tag{19}$$

where K_{di} is the elastic modulus of the spring and C_{0i} is the coefficient of viscosity. The parameters K_{di} and C_{0i} are parts of the uncertain parameter vector $\underline{\theta}$.

IV. RESULTS

The parameters $\underline{\theta}$ are associated with the structural parameters introduced in the model equations (16) and (19). The correspondence of the parameters in the set $\underline{\theta}$ and the parameters in the model equations (16) and (19) is given in Table 1. Specifically the first six parameters are associated with the sliding friction isolators located at the left and right edge of the bridge deck, while the next four the parameters are associated with the two model parameters of the viscous dampers at the left and right edge of the bridge deck. The nominal values of the model parameters in (16) and (19) are set to the ones obtained by calibrating the models using measurements from component tests [7]. The parameters $\underline{\theta}$ scale the nominal values of the properties that they model so that the value of the parameters equal to one corresponds to the nominal values of the isolator parameters in the nonlinear models (16) and (19). The parameters of the rubber devices in equation (18) are kept fixed to their nominal values. The data set D is constituted from experimental measurements of bearing displacement, pier total isolator force, pier drift, pier shear force, and pier acceleration obtained during the shake table tests of the combined bridge-isolators system.

Table 1. Definition of the parameters in the set $\underline{\theta}$.

Parameter definitions		
Parameter	***Type***	***Parameter in (16) or (19)***
θ_1	Friction	$f_{\min,1}$
θ_2	Friction	Δf_1
θ_3	Friction	a_1
θ_4	Friction	$f_{\min,2}$
θ_5	Friction	Δf_2
θ_6	Friction	a_2
θ_7	Damper	K_{d1}
θ_8	Damper	C_{01}
θ_9	Damper	K_{d2}
θ_{10}	Damper	C_{02}

The parallelized TMCMC [4] is used to draw samples from the importance region of the posterior probability density function. Parameter estimation results were obtained with 1000 samples per stage in the TMCMC algorithm and eight computer workers were used to perform in parallel the computations involved in the TMCMC algorithm. The number of stages required to compute the solution is of the order of 20 to 25. The computer programming environment where the model is implemented is also of great importance since it plays a crucial role in the time required to perform a model evaluation for a specific set of parameters, which is required by the stochastic simulation algorithms. In this work, the structural model is implemented in the Fortran programming language which enables it to be very fast and efficient for use in the TMCMC algorithm. The computational time for each simulation of the system is approximately 10 seconds, resulting in a time-to-solution of the order of several hours.

Fig. 5 (left) shows the uncertainty in the marginal distributions of the 10 model parameters on the friction and damping models (16) and (19), respectively. Parameter number 11 is the prediction error parameter σ, which was assumed to be the same for all the measured response time histories. The measures of fit $J_j(\underline{\theta})$, $j = 1, \ldots, 6$, between the measured response

time histories and the model predicted response time histories for the TMCMC samples are given in Fig. 5 (right), along with the statistics (5% quantile, mean - std, mean, mean + std, 5% quantile) computed from the propagating TMCMC samples. The marginal distributions of the parameters are demonstrated in Fig. 6.

It is clear from these figures that uncertainties in the model parameters vary from 5% level to as high as 50% for the damping coefficient C_{01} for the viscous damper model. The marginal distributions of the parameters Δf_1 and Δf_2 of the sliding friction models are estimated to be bimodal for both friction devices. These uncertainties are expected to affect the predictions of various response quantities of interest that are critical to the performance of such systems. From Fig. 5 (right) it can be seen that compared to the nominal nonlinear models there is a reduction in the error between the experimental time histories and the time histories predicted by the calibrated models. This reduction varies from 5% to 30% depending the measured response quantity considered.

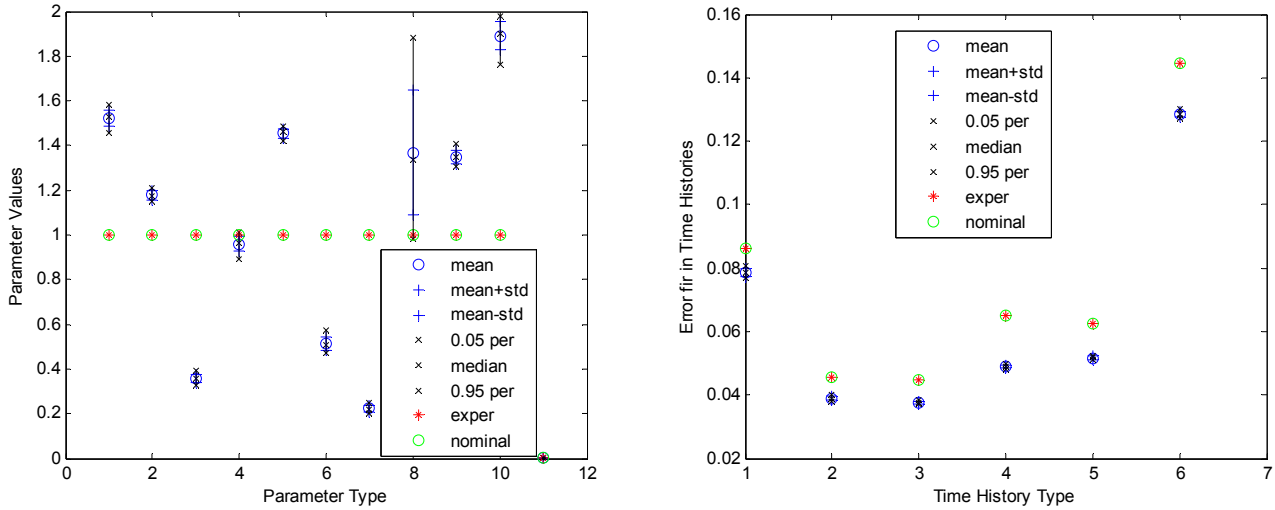

Figure 5. *Left:* Calibrated model parameter values. *Right:* Fit with experimental time histories.

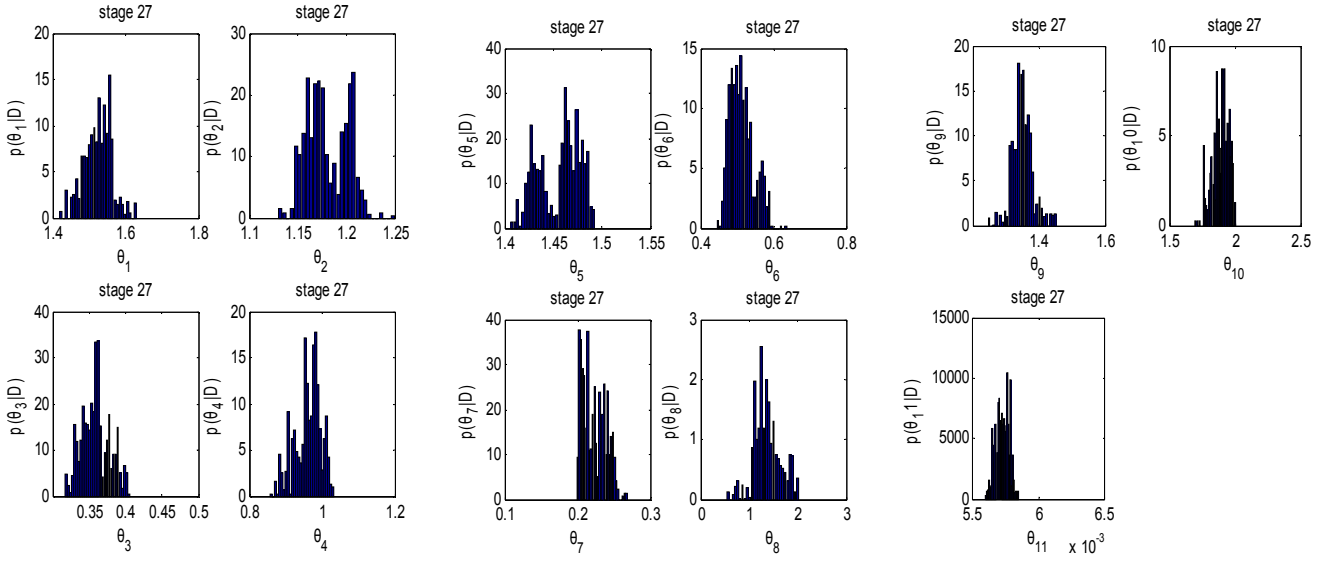

Figure 6. Marginal distributions of the uncertain model parameters.

The uncertainties of the model parameters are propagated through the model to estimate the uncertainties in the output response time histories. This was achieved by using the samples drawn from the posterior probability density function to estimate the mean and standard deviation of a function of the uncertain parameters, using (12) and (13). The robust model predicted time histories are compared with the experimental measurements in Fig. 7 for four selected response quantities of interest. It is observed that the model predictions adequately fit the measured time histories for all response time histories considered in the calibration. Discrepancies between the experimental measurements and the robust model predictions for the

isolator displacement could be attributed to the inadequacy of the isolator models to capture all characteristics of the isolator devices. Also it should be observed that the uncertainty in the predictions of the response time histories is very small compared to the uncertainty in the model parameters shown in Fig. 5 (left) and Figure 6.

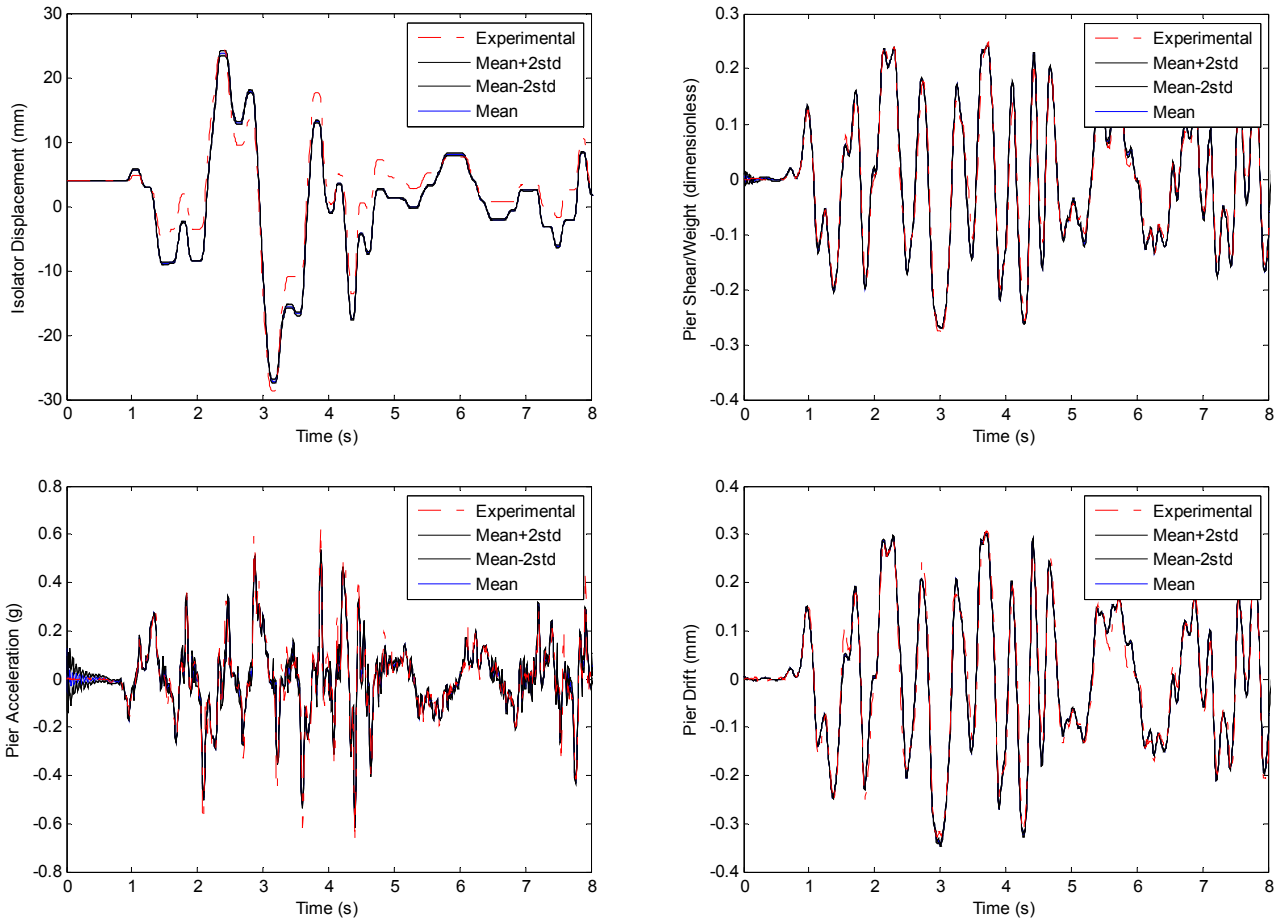

Figure 7. Uncertainty propagation: Response uncertainty along with experimental data. Isolator Displacement, Pier Shear force, Pier Acceleration, Pier Drift.

V. Conclusion

A Bayesian uncertainty quantification and propagation framework was presented for estimating the parameters of nonlinear models using response time history measurements. The framework was applied to calibrate the parameters of the nonlinear models involved for representing the behavior of a seismically isolated bridge using experimentally measured response time histories. Stochastic simulation algorithms were used to estimate the uncertainty in the model parameters and propagate through the model to estimate the quality in the fit between the model predicted and measured response time histories. It is found that the identified values of the model parameters are different from the nominal values obtained by calibration procedures at the component level using component tests. This introduces the need for calibrating the model parameters taking into account component and system tests simultaneously. The nonlinear models introduced for the three types of isolator devises are adequate to represent the behavior of the isolated bridge since there is a very good match between the model predicted responses with the measured responses considered in the Bayesian parameter estimation. Also, the uncertainty in the model parameters is significant for some of the isolator devices. This is expected to affect uncertainties in predictions of critical response quantities of interest. The theoretical and computational developments used in this work can be used to identify and propagate uncertainties in large order nonlinear systems consisting of linear and nonlinear components.

ACKNOWLEDGMENT

This research has been implemented under the ”ARISTEIA” Action of the ”Operational Programme Education and Lifelong Learning” and was co-funded by the European Social Fund (ESF) and Greek National Resources.

REFERENCES

[1] C. Papadimitriou, J.L. Beck, L.S. Katafygiotis, "Updating robust reliability using structural test data," Probabilist Eng Mech, 16 (2001) 103-113.
[2] L. Tierney, J.B. Kadane, "Accurate Approximations for Posterior Moments and Marginal Densities," J Am Stat Assoc, 81 (1986) 82-86.
[3] J.Y. Ching, Y.C. Chen, "Transitional markov chain monte carlo method for Bayesian model updating, model class selection, and model averaging," J Eng Mech-Asce, 133 (2007) 816-832.
[4] P. Angelikopoulos, C. Papadimitriou, P. Koumoutsakos, "Bayesian uncertainty quantification and propagation in molecular dynamics simulations: A high performance computing framework," J Chem Phys, 137 (2012).
[5] J.L. Beck, L.S. Katafygiotis," Updating models and their uncertainties. I: Bayesian statistical framework," J Eng Mech-Asce, 124 (1998) 455-461.
[6] K.V. Yuen, "Bayesian Methods for Structural Dynamics and Civil Engineering," John Wiley & Sons, Singapore, 2010.
[7] P. Tsopelas, S. Okamoto, M.C. Constantinou, D. Ozaki, S. Fujii, "NCEER-TAISEI Corporation Research Program on Sliding Seismic Isolation Systems for Bridges - Experimental and Analytical Study of Systems Consisting of Sliding Bearings, Rubber Restoring Force Devices and Fluid Dampers," Report No. NCEER 94-0002. NAT. CTR. for Earthquake Engrg. Res., State University of New York, Buffalo, NY, (1994).